

Bottomonium suppression at RHIC and LHC

Michael Strickland

Kent State University
Kent, OH USA

N. Brambilla, M.-A. Escobedo, MS, A. Vairo, P. Vander Griend,
and J.H. Weber, 2012.01240 and 2107.06222

H. Ba Omar, M. Escobedo, A. Islam, MS, S. Thapa, P. Vander Griend,
and J. Weber, 2107.06147 (open-source Qtraj 1.0 code release)

N. Brambilla, M.-A. Escobedo, A. Islam, MS, A. Tiwari, A. Vairo, P. Vander Griend, 2205.10289

RBRC Workshop - Predictions for sPHENIX
21 July 2022



U.S. DEPARTMENT OF
ENERGY



Ohio Supercomputer Center
An OH·TECH Consortium Member

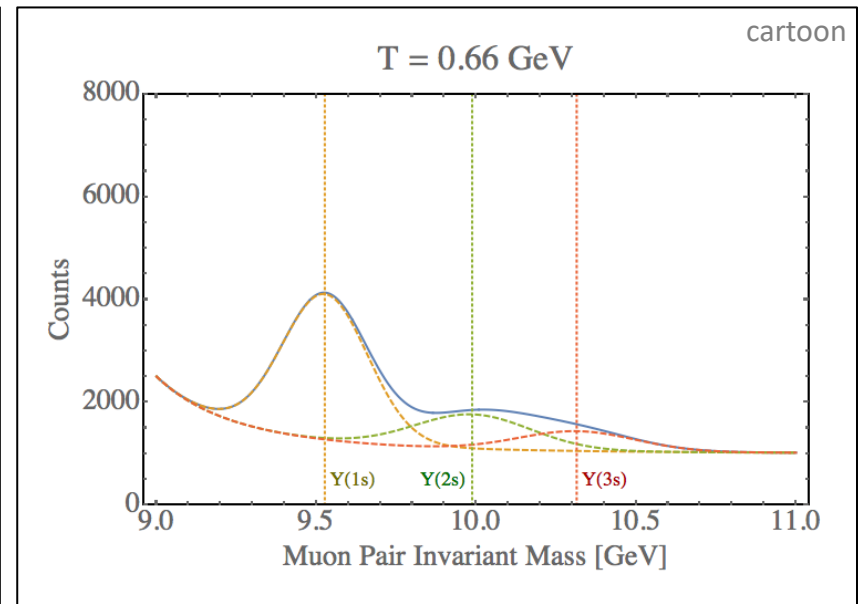
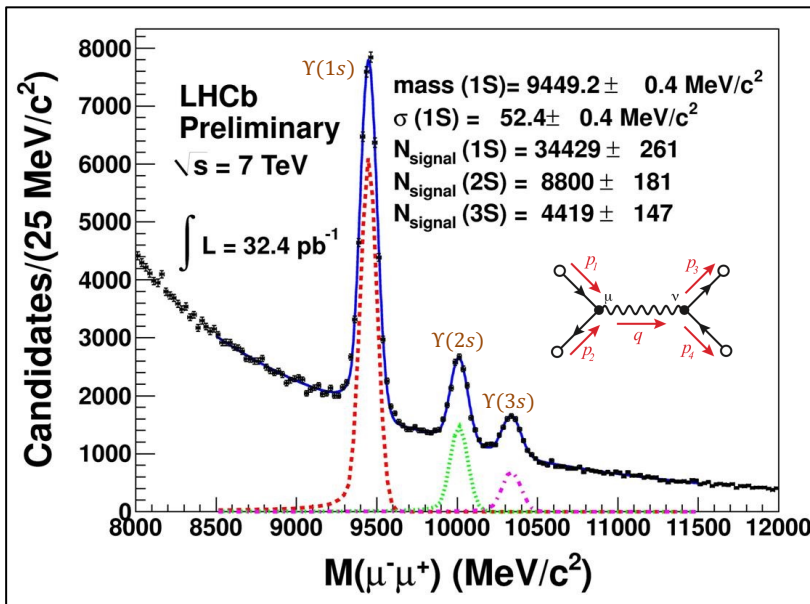
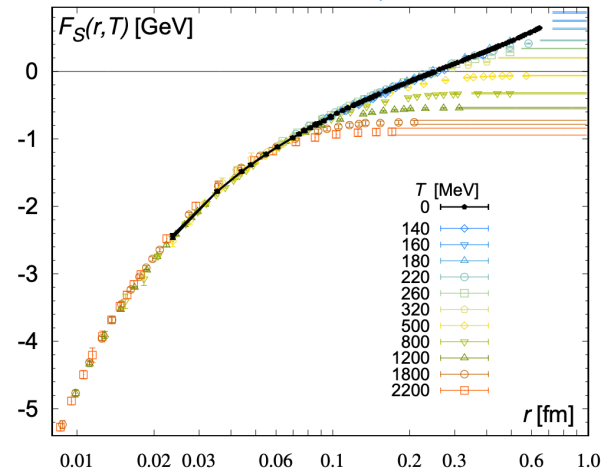
Bottomonium Suppression

- In a high temperature quark-gluon plasma we expect **weaker color binding** (Debye screening + asymptotic freedom)

E. V. Shuryak, Phys. Rept. 61, 71–158 (1980)
 T. Matsui, and H. Satz, Phys. Lett. B178, 416 (1986)
 F. Karsch, M. T. Mehr, and H. Satz, Z. Phys. C37, 617 (1988)

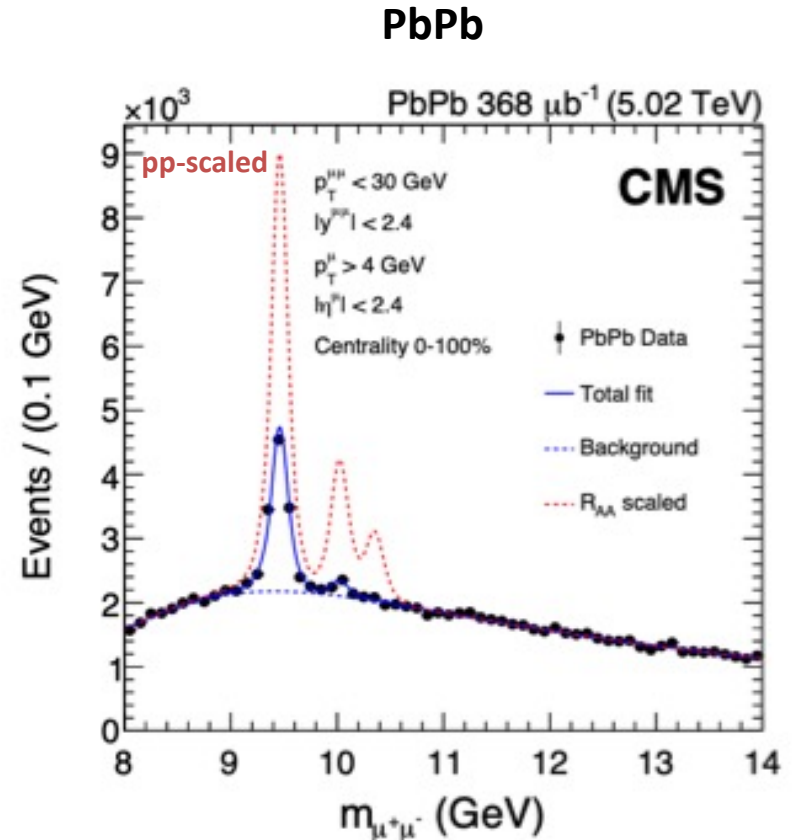
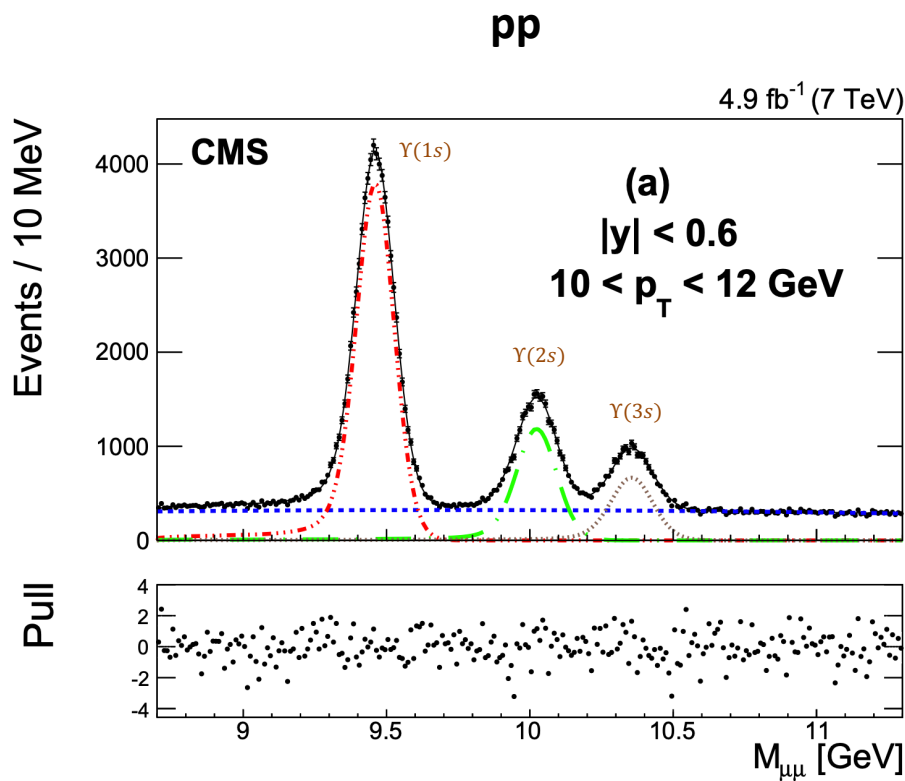
- Also, high energy plasma particles which slam into the bound states cause them to have shorter lifetimes → **larger spectral widths**

TUMQCD Collaboration, 1804.10600

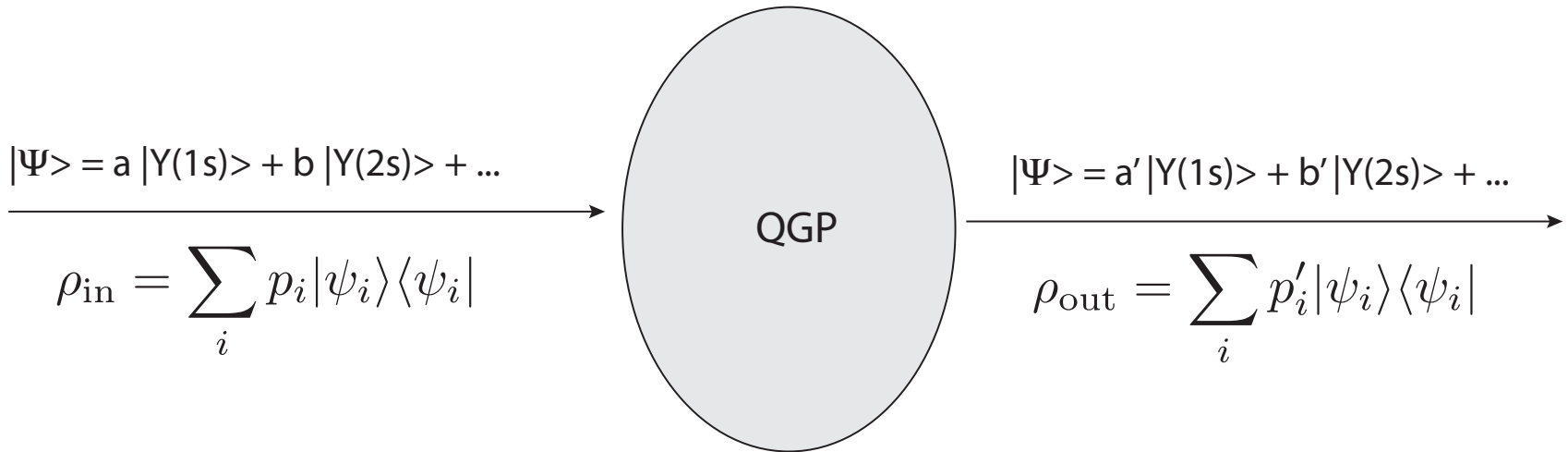


Experimental data – 5.02 TeV Dimuon Spectra

The **CMS**, **ALICE**, and **ATLAS** experiments have measured bottomonium production in both pp and Pb-Pb collisions at 5.02 TeV. Here I show CMS results.

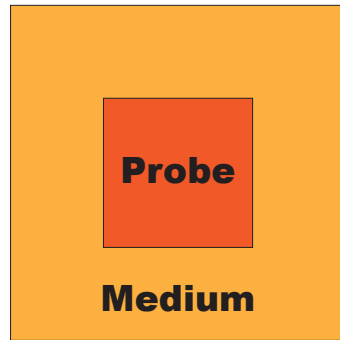


Conceptual problem



- Bottomonium states have a large binding energy ($1S \sim 1 \text{ GeV}$) and are produced locally (hard processes) at early times in hard collisions ($t < 1 \text{ fm}/c$).
- They then propagate through the plasma and interact with the medium.
- Bound states can break up and potentially re-form due to in-medium transitions induced by in-medium gluon absorption and emission.

Open quantum system (OQS) approach



Probe = heavy-quarkonium state

Medium = light quarks and gluons that comprise the QGP

- Can treat heavy quarkonium states propagating through QGP using an open quantum system approach

$$H_{\text{tot}} = H_{\text{probe}} \otimes I_{\text{medium}} + I_{\text{probe}} \otimes H_{\text{medium}} + H_{\text{int}}$$

- Total density matrix

$$\rho_{\text{tot}} = \sum_j p_j |\psi_j\rangle\langle\psi_j| \longrightarrow \frac{d}{dt}\rho_{\text{tot}} = -i[H_{\text{tot}}, \rho_{\text{tot}}]$$

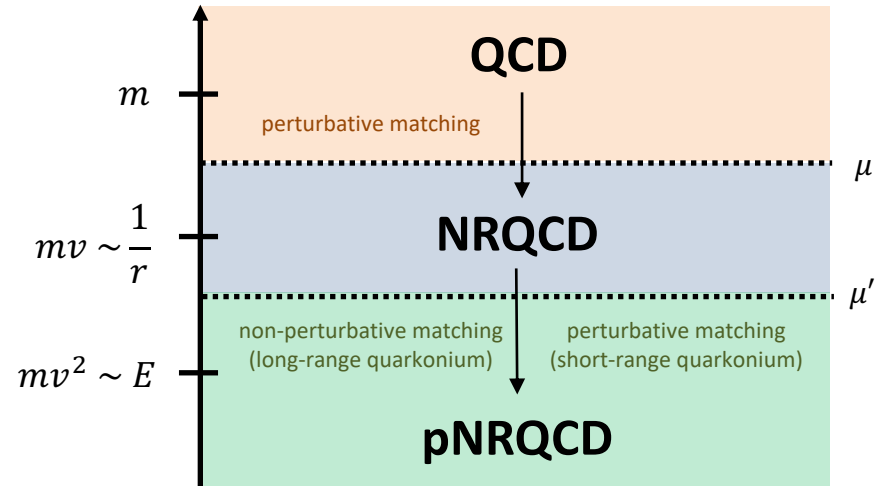
- Reduced density matrix (medium dof integrated out)

$$\rho_{\text{probe}} = \text{Tr}_{\text{medium}}[\rho_{\text{tot}}] \longrightarrow \text{“Master equation”}$$

OQS + pNRQCD \rightarrow Lindblad equation

- What are the relevant scales?

- Temperature T
- Bound state mass $m \gg T$
- Bound state size $r \sim 1/mv \sim a_0$ (Bohr radius)
- Debye mass m_D
- Binding energy $E \sim mv^2$



- Separation of time scales

- Medium relaxation time scale $\langle \hat{O}_M(t) \hat{O}_M(0) \rangle \sim e^{-t/t_M} \rightarrow \frac{1}{T}$
- Intrinsic probe time scale $t_P \sim \frac{1}{\omega_i - \omega_j} \rightarrow \frac{1}{E}$
- Probe relaxation time scale $\langle p(t) \rangle \sim e^{-t/t_{\text{rel}}} \rightarrow \frac{1}{\text{self-energy}} \sim \frac{1}{\alpha_s a_0^2 \Lambda^3} \quad \Lambda = T, E$

$$\frac{1/r \gg T \sim m_D \gg E}{t_{\text{rel}}, t_P \gg t_M} \rightarrow$$

$$\frac{d\rho_{\text{probe}}}{dt} = -i[H_{\text{probe}}, \rho_{\text{probe}}] + \sum_n \left(C_n \rho_{\text{probe}} C_n^\dagger - \frac{1}{2} \{C_n^\dagger C_n, \rho_{\text{probe}}\} \right)$$

N. Brambilla, M. A. Escobedo, J. Soto and A. Vairo, 1612.07248, 1711.04515

OQS + pNRQCD – Lindblad reorganization

$$\frac{d\rho_{\text{probe}}}{dt} = -i[H_{\text{probe}}, \rho_{\text{probe}}] + \sum_n \left(C_n \rho_{\text{probe}} C_n^\dagger - \frac{1}{2} \{C_n^\dagger C_n, \rho_{\text{probe}}\} \right)$$

- H_{probe} is Hermitian (includes singlet and octet states)
- C_n are the **collapse (or jump) operators** (connect different internal states)
- Partial and **total decay width operators** are

$$\Gamma_n = C_n^\dagger C_n \quad \Gamma = \sum_n \Gamma_n$$

- Can reorganize Lindblad equation by defining

$$H_{\text{eff}} = H_{\text{probe}} - \frac{i}{2} \Gamma$$

← Non-Hermitian effective Hamiltonian

$$\longrightarrow \frac{d\rho_{\text{probe}}}{dt} = -iH_{\text{eff}}\rho_{\text{probe}} + i\rho_{\text{probe}}H_{\text{eff}}^\dagger + \sum_n C_n \rho_{\text{probe}} C_n^\dagger$$

LO OQS + pNRQCD Hamiltonian and collapse operators

N. Brambilla, M. A. Escobedo, J. Soto and A. Vairo, 1612.07248, 1711.04515

$$\frac{d\rho_{\text{probe}}}{dt} = -iH_{\text{eff}}\rho_{\text{probe}} + i\rho_{\text{probe}}H_{\text{eff}}^\dagger + \sum_n C_n \rho_{\text{probe}} C_n^\dagger$$

$$\rho = \begin{pmatrix} \rho_s & 0 \\ 0 & \rho_o \end{pmatrix}$$

$$H_{\text{probe}} = \begin{pmatrix} h_s & 0 \\ 0 & h_o \end{pmatrix} + \frac{r^2}{2} \gamma \begin{pmatrix} 1 & 0 \\ 0 & \frac{N_c^2 - 2}{2(N_c^2 - 1)} \end{pmatrix}$$

mass shift

$$C_i^0 = \sqrt{\frac{\kappa}{N_c^2 - 1}} r^i \begin{pmatrix} 0 & 1 \\ \sqrt{N_c^2 - 1} & 0 \end{pmatrix},$$

$$\Gamma = \kappa r^i \begin{pmatrix} 1 & 0 \\ 0 & \frac{N_c^2 - 2}{2(N_c^2 - 1)} \end{pmatrix} r^i$$

Total width $\rightarrow \text{Im}[V]$
 $H_{\text{eff}} = H_{\text{probe}} - \frac{i}{2}\Gamma$

$$C_i^1 = \sqrt{\frac{(N_c^2 - 4)\kappa}{2(N_c^2 - 1)}} r^i \begin{pmatrix} 0 & 0 \\ 0 & 1 \end{pmatrix}.$$

$$\gamma \equiv \frac{g^2}{6 N_c} \text{Im} \int_{-\infty}^{+\infty} ds \langle T E^{a,i}(s, \mathbf{0}) E^{a,i}(0, \mathbf{0}) \rangle$$

$$\kappa \equiv \frac{g^2}{6 N_c} \text{Re} \int_{-\infty}^{+\infty} ds \langle T E^{a,i}(s, \mathbf{0}) E^{a,i}(0, \mathbf{0}) \rangle$$

- Six collapse operators cover**
- singlet \rightarrow octet,
 - octet \rightarrow singlet
 - octet \rightarrow octet

LO OQS + pNRQCD Hamiltonian and collapse operators

N. Brambilla, M. A. Escobedo, J. Soto and A. Vairo, 1612.07248, 1711.04515

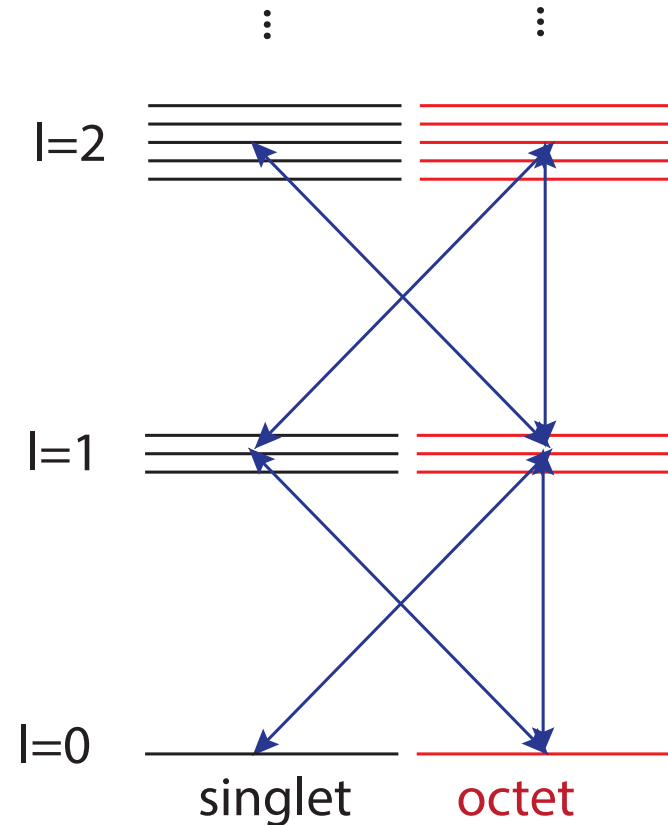
$$\frac{d\rho_{\text{probe}}}{dt} = -iH_{\text{eff}}\rho_{\text{probe}} + i\rho_{\text{probe}}H_{\text{eff}}^\dagger + \sum_n C_n \rho_{\text{probe}} C_n^\dagger$$

$$\rho = \begin{pmatrix} \rho_s & 0 \\ 0 & \rho_o \end{pmatrix}$$

$$C_i^0 = \sqrt{\frac{\kappa}{N_c^2 - 1}} r^i \begin{pmatrix} 0 & 1 \\ \sqrt{N_c^2 - 1} & 0 \end{pmatrix},$$

$$C_i^1 = \sqrt{\frac{(N_c^2 - 4)\kappa}{2(N_c^2 - 1)}} r^i \begin{pmatrix} 0 & 0 \\ 0 & 1 \end{pmatrix}.$$

- Six collapse operators cover**
- singlet \rightarrow octet,
 - octet \rightarrow singlet
 - octet \rightarrow octet



LO OQS + pNRQCD Hamiltonian and collapse operators

N. Brambilla, M. A. Escobedo, J. Soto and A. Vairo, 1612.07248, 1711.04515

$$\frac{d\rho_{\text{probe}}}{dt} = -iH_{\text{eff}}\rho_{\text{probe}} + i\rho_{\text{probe}}H_{\text{eff}}^\dagger + \sum_n C_n \rho_{\text{probe}} C_n^\dagger$$

$$\rho = \begin{pmatrix} \rho_s & 0 \\ 0 & \rho_o \end{pmatrix}$$

$$H_{\text{probe}} = \begin{pmatrix} h_s & 0 \\ 0 & h_o \end{pmatrix} + \frac{r^2}{2} \gamma \begin{pmatrix} 1 & 0 \\ 0 & \frac{N_c^2 - 2}{2(N_c^2 - 1)} \end{pmatrix}$$

$$C_i^0 = \sqrt{\frac{\kappa}{N_c^2 - 1}} r^i \begin{pmatrix} 0 & 1 \\ \sqrt{N_c^2 - 1} & 0 \end{pmatrix},$$

$$\Gamma = \kappa r^i \begin{pmatrix} 1 & 0 \\ 0 & \frac{N_c^2 - 2}{2(N_c^2 - 1)} \end{pmatrix} r^i$$

Total width $\rightarrow \text{Im}[V]$
 $H_{\text{eff}} = H_{\text{probe}} - \frac{i}{2}\Gamma$

$$C_i^1 = \sqrt{\frac{(N_c^2 - 4)\kappa}{2(N_c^2 - 1)}} r^i \begin{pmatrix} 0 & 0 \\ 0 & 1 \end{pmatrix}.$$

$$\gamma \equiv \frac{g^2}{6 N_c} \text{Im} \int_{-\infty}^{+\infty} ds \langle T E^{a,i}(s, \mathbf{0}) E^{a,i}(0, \mathbf{0}) \rangle$$

$$\kappa \equiv \frac{g^2}{6 N_c} \text{Re} \int_{-\infty}^{+\infty} ds \langle T E^{a,i}(s, \mathbf{0}) E^{a,i}(0, \mathbf{0}) \rangle$$

- Six collapse operators cover**
- singlet \rightarrow octet,
 - octet \rightarrow singlet
 - octet \rightarrow octet

Going beyond leading order in E/T

N. Brambilla, M.-A. Escobedo, A. Islam, M.S., A. Tiwari, A. Vairo, P. Vander Griend, 2205.10289

- Results on previous slides were obtained by truncating at leading order (NLO) in E/T (binding energy over temperature). This was extended to NLO in the reference above.
- By decomposing states into radial and angular components, for an isotropic system we can rewrite the operators as acting only on the 1d effective wavefunction $u(r) = r R(r,t)$.

- At NLO, there are six jump operators (shown on the right).

$$C_{s \rightarrow o}^{\uparrow} = r - \frac{N_c \alpha_s}{8T} + \frac{1}{2MT} \left(\frac{\partial}{\partial r} - \frac{l+1}{r} \right),$$

$$C_{s \rightarrow o}^{\downarrow} = r - \frac{N_c \alpha_s}{8T} + \frac{1}{2MT} \left(\frac{\partial}{\partial r} + \frac{l}{r} \right),$$

$$C_{o \rightarrow s}^{\uparrow} = r + \frac{N_c \alpha_s}{8T} + \frac{1}{2MT} \left(\frac{\partial}{\partial r} - \frac{l+1}{r} \right),$$

$$C_{o \rightarrow s}^{\downarrow} = r + \frac{N_c \alpha_s}{8T} + \frac{1}{2MT} \left(\frac{\partial}{\partial r} + \frac{l}{r} \right),$$

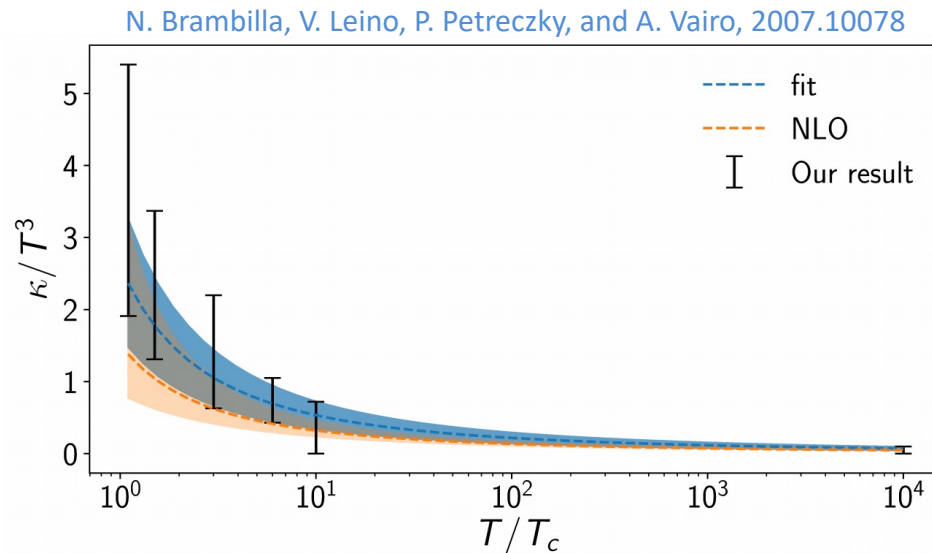
$$C_{o \rightarrow o}^{\uparrow} = r + \frac{1}{2MT} \left(\frac{\partial}{\partial r} - \frac{l+1}{r} \right),$$

$$C_{o \rightarrow o}^{\downarrow} = r + \frac{1}{2MT} \left(\frac{\partial}{\partial r} + \frac{l}{r} \right).$$

Values of $\hat{\kappa}$ and $\hat{\gamma}$ used

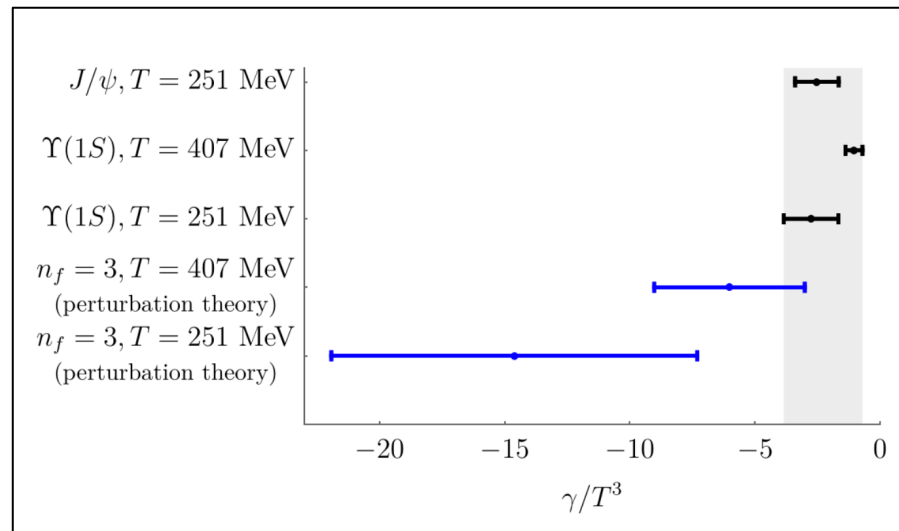
- We used NLO fits to recent lattice measurements of the heavy quark transport coefficient $\hat{\kappa} \equiv \kappa/T^3$. Note that this is related to the heavy quark diffusion constant D .

- N. Brambilla, V. Leino, P. Petreczky, and A. Vairo, 2007.10078



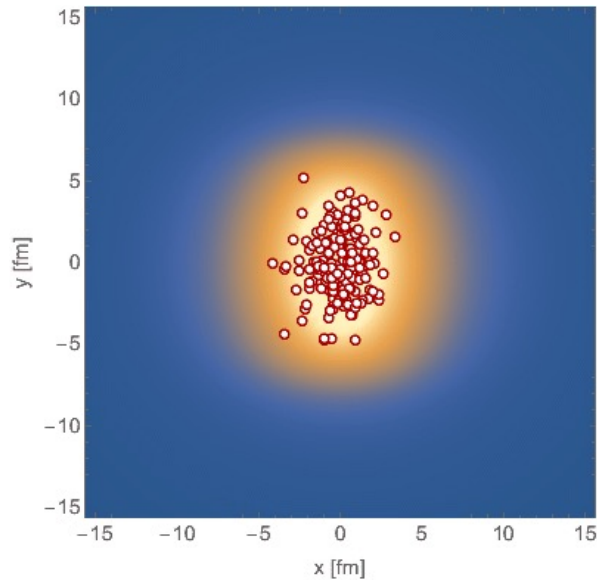
- The value of $\hat{\gamma} \equiv \gamma/T^3$ is less constrained, we vary it in the range $-3.5 < \hat{\gamma} < 0$.

- N. Brambilla, M. A. Escobedo, J. Soto and A. Vairo, 1612.07248.
- N. Brambilla, M. A. Escobedo, J. Soto and A. Vairo, 1711.04515.
- N. Brambilla, M. A. Escobedo, A. Vairo and P. Vander Griend, 1903.08063.



N. Brambilla, M. A. Escobedo, A. Vairo and P. Vander Griend, 1903.08063.

Computing survival probabilities with QTraj



- We sampled bottomonium production points and initial COM transverse momentum using **Monte-Carlo sampling** (physical trajectories).
- Temperature evolution provided **by 3+1D anisotropic hydrodynamics** (good description of identified soft hadron spectra and anisotropic flow, see backup slides).
- Along each physical trajectory, we solved the **real-time 3D Schrödinger equation with a complex potential and stochastically sampled jumps** → Lindblad equation.
- We then solved for the **survival probability** of S- and P-wave states (see box to the left).

Survival probability

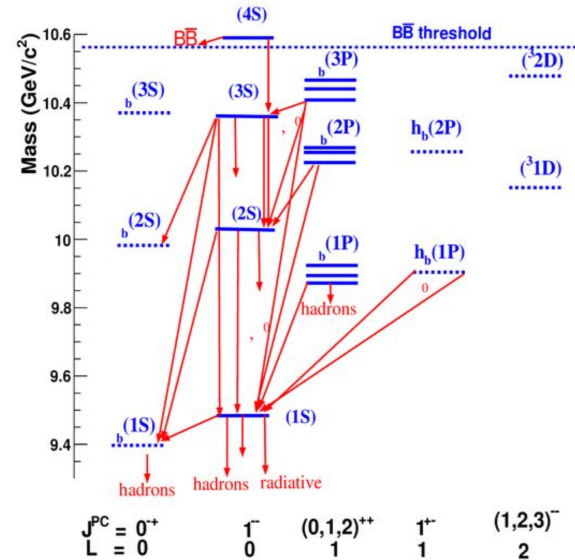
$$SP(n, l) = \frac{|\langle n, l | \psi(t_f) \rangle|^2}{|\langle n, l | \psi(t_0) \rangle|^2}$$

- Used $N = 4096$ points
- $L = 108 a_0$
- $\Delta t = 2 \times 10^{-4}$ fm

Feed-down implementation

$$\vec{N}_{\text{observed}} = F \vec{N}_{\text{direct}}$$

$$F = \begin{pmatrix} 1 & 0.2645 & 0.0194 & 0.352 & 0.18 & 0.0657 & 0.0038 & 0.1153 & 0.077 \\ 0 & 1 & 0 & 0 & 0 & 0.106 & 0.0138 & 0.181 & 0.089 \\ 0 & 0 & 1 & 0 & 0 & 0 & 0 & 0 & 0 \\ 0 & 0 & 0 & 1 & 0 & 0 & 0 & 0.0091 & 0 \\ 0 & 0 & 0 & 0 & 1 & 0 & 0 & 0 & 0.0051 \\ 0 & 0 & 0 & 0 & 0 & 1 & 0 & 0 & 0 \\ 0 & 0 & 0 & 0 & 0 & 0 & 1 & 0 & 0 \\ 0 & 0 & 0 & 0 & 0 & 0 & 0 & 1 & 0 \\ 0 & 0 & 0 & 0 & 0 & 0 & 0 & 0 & 1 \end{pmatrix}$$

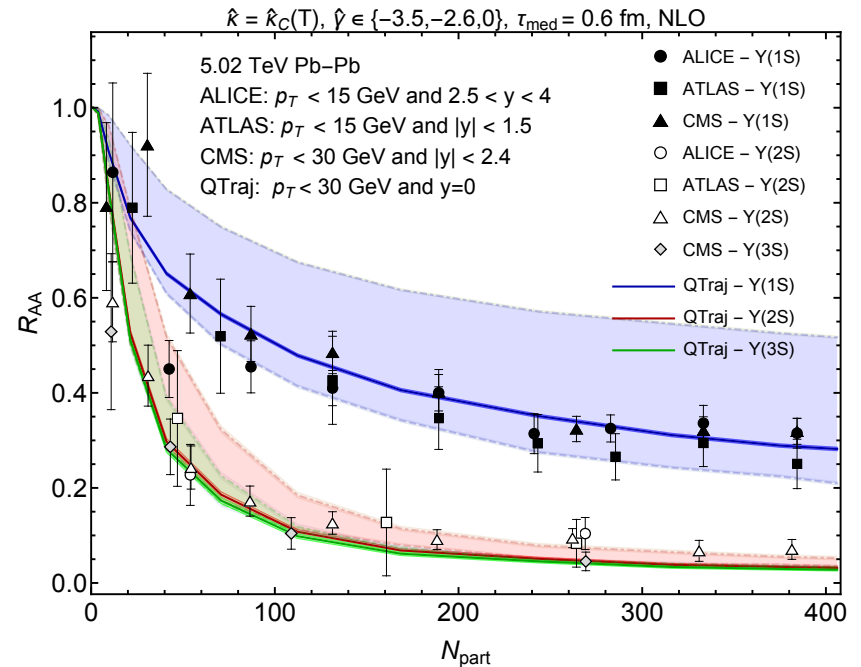
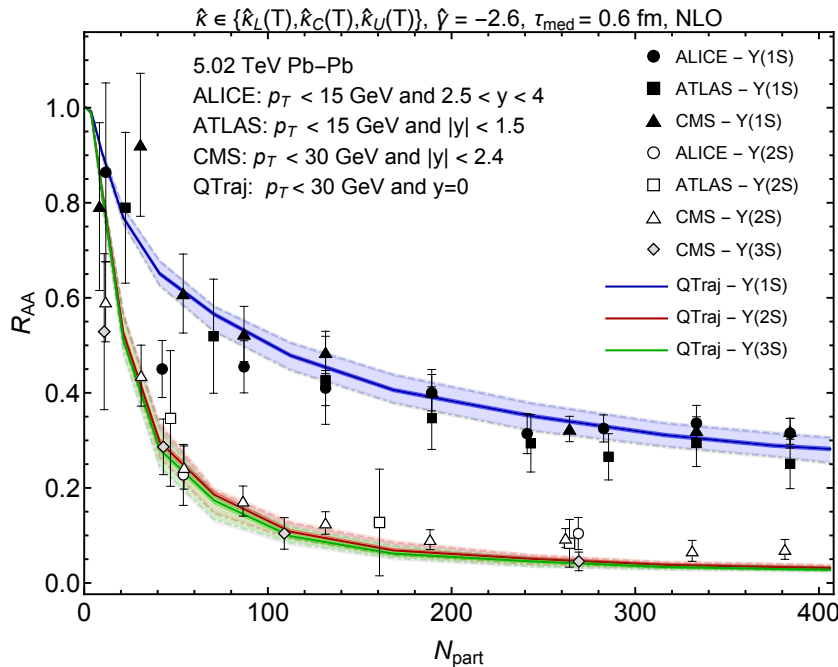


- N_{direct} corresponds to $(N_{1S}, N_{2S}, N_{1P} \times 3, N_{3S}, N_{2P} \times 3, N_{2D})^T$ where, e.g., N_{1S} is the final number of $Y(1S)$ states that can decay in the dilepton channel.
- N_{direct} can be obtained using $\langle N_{\text{bin}}(b) \rangle * \sigma_{\text{direct}} * (\text{Survival probability})$
- After feed down, we then normalize by the pp collision result scaled to AA $\rightarrow R_{AA}$.

$$R_{AA}^i(c) = \frac{(F \cdot S(c) \cdot \vec{\sigma}_{\text{direct}})^i}{\sigma_{\text{exp}}^i}$$

NLO OQS + pNRQCD predictions for R_{AA} vs N_{part} at LHC

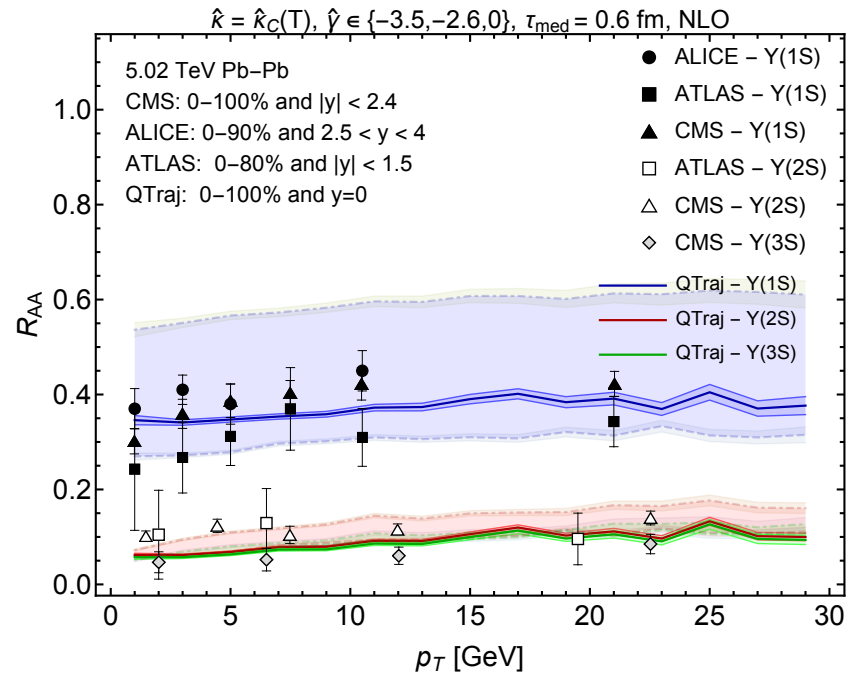
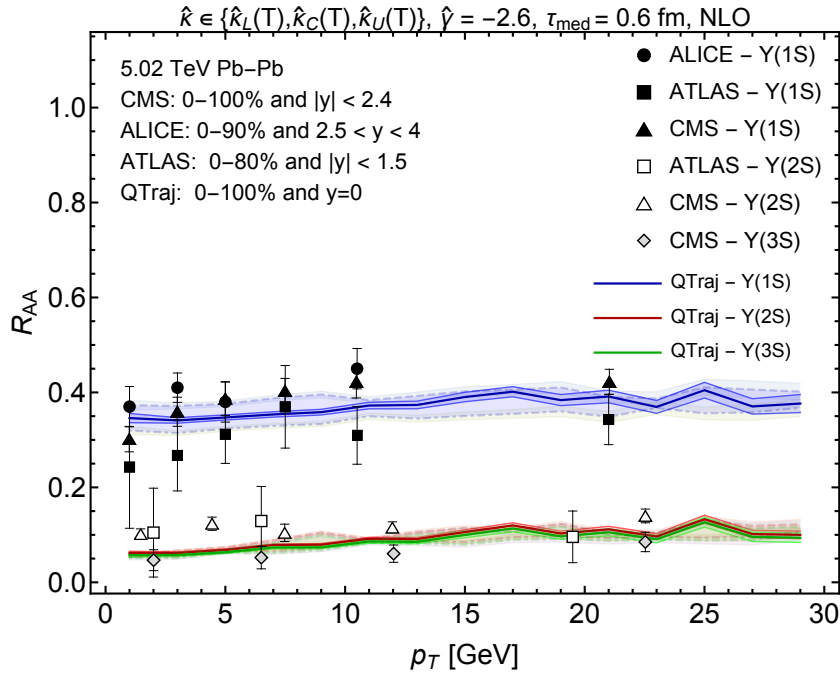
N. Brambilla, M.-A. Escobedo, A. Islam, M.S., A. Tiwari, A. Vairo, P. Vander Griend, 2205.10289



- **Left panel:** Result including feed down, when varying \hat{k} over the theoretical uncertainty.
- **Right panel:** Result including feed down, when varying \hat{y} over the theoretical uncertainty
- **Note:** The NLO results above ignore jumps (H_{eff} only). The effect of jumps is expected to be small based on prior studies, but requires lots of computer time (forthcoming).
- The statistical uncertainty associated with the average over physical trajectories is on the order of the line width.

R_{AA} vs transverse momentum

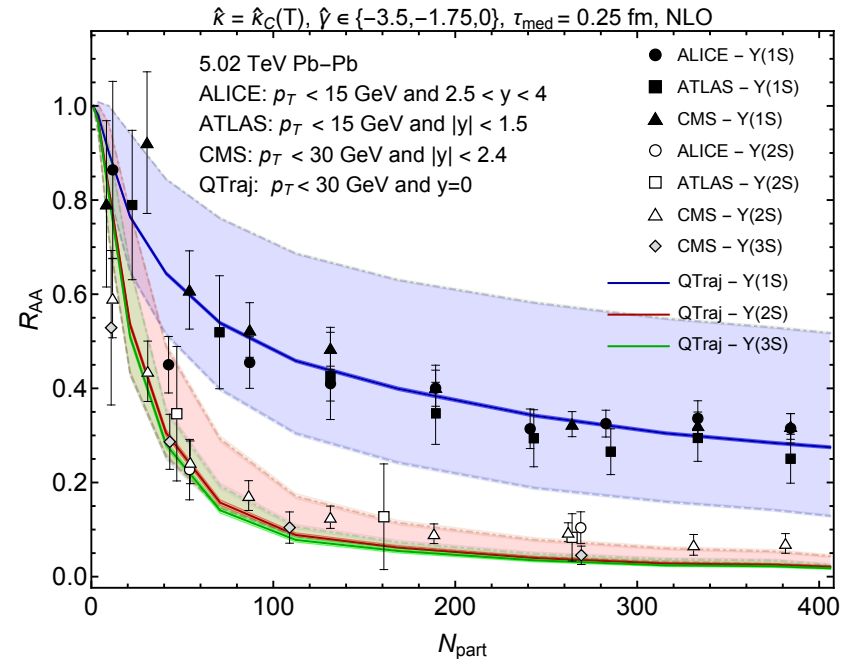
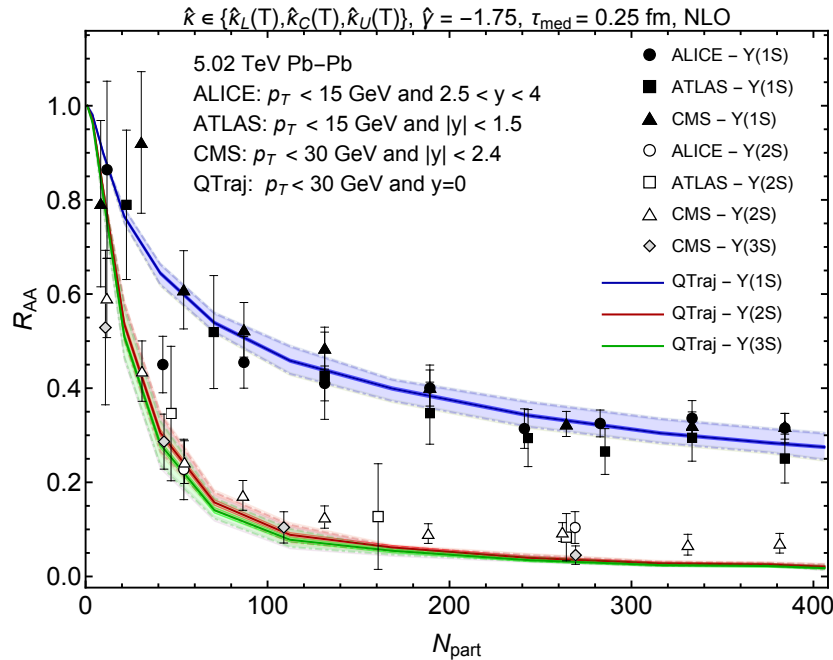
N. Brambilla, M.-A. Escobedo, A. Islam, M.S., A. Tiwari, A. Vairo, P. Vander Griend, 2205.10289



- QTraj predictions consistent with experimental observations.
- Very flat. Small decrease comes from longer time spent in the QGP as the velocity decreases.
- Once again, larger variation from uncertainty in \hat{y} .

NLO OQS + pNRQCD predictions for R_{AA} vs N_{part} at LHC

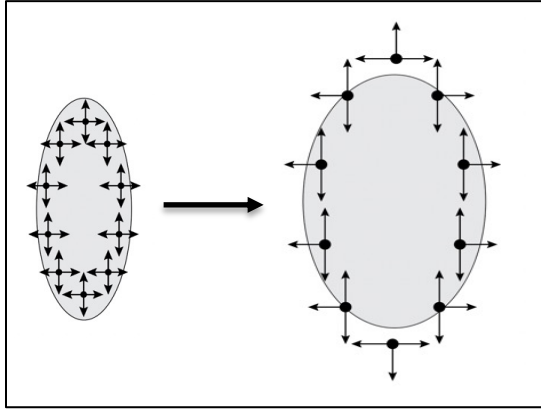
N. Brambilla, M.-A. Escobedo, A. Islam, M.S., A. Tiwari, A. Vairo, P. Vander Griend, 2205.10289



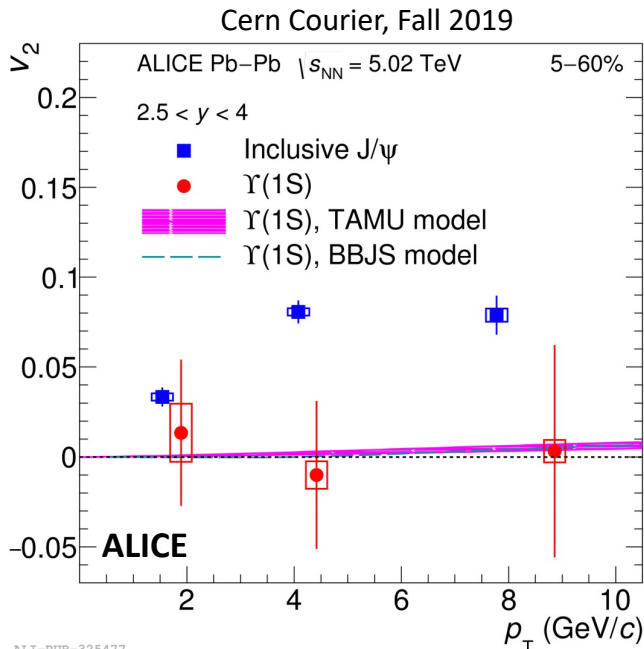
- Note that It is possible to use a shorter medium initialization time and obtain a similar description of the data.
- Above shows results using $\tau_{med} = 0.25$ fm rather than 0.6 fm
- In this case, I changed the central value of gamma plotted, but the range of variation is the same.

Momentum-space anisotropies

4d flow tomography



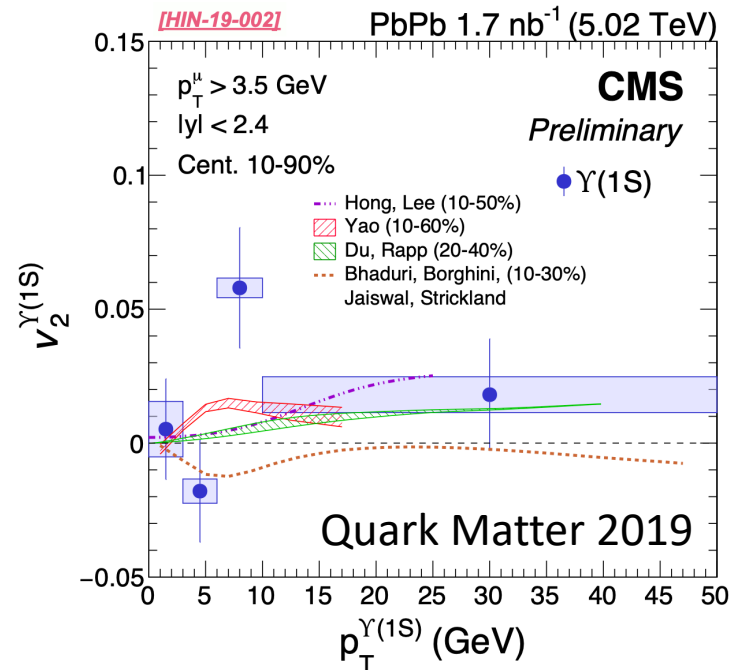
- Bottomonium probably doesn't flow in the "collective flow" sense.
- However, there can be momentum-space anisotropies induced by path-length differences in suppression along the short and long sides of the QGP.



ALI-PUB-325477

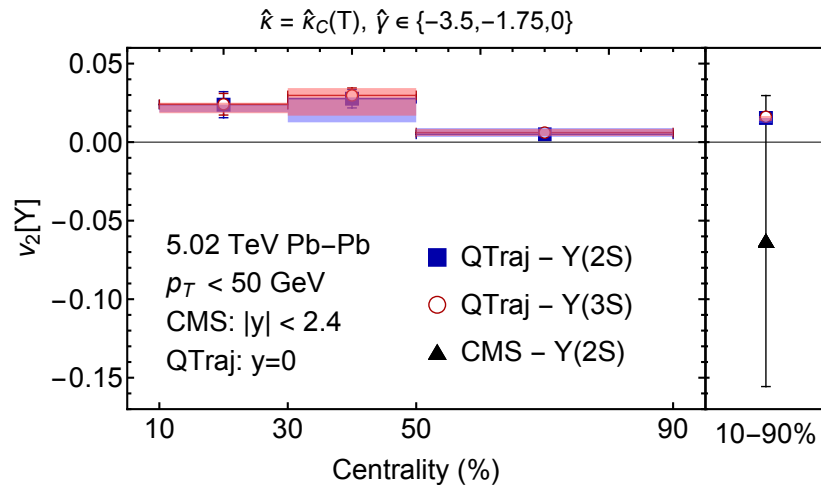
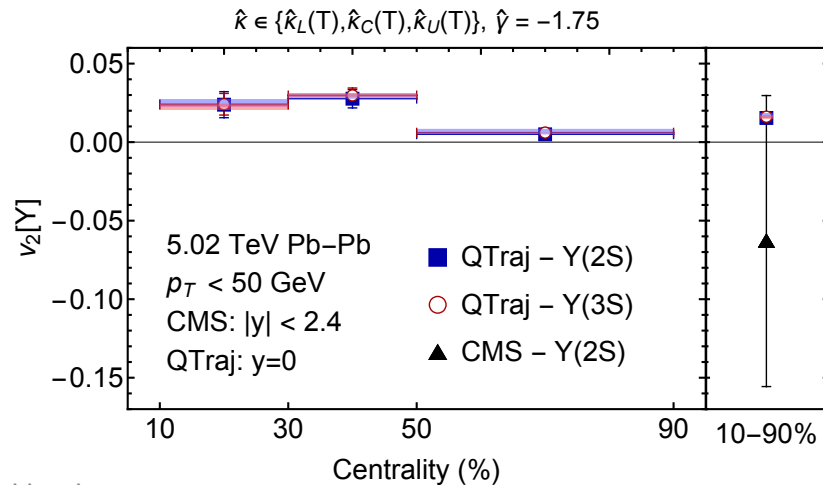
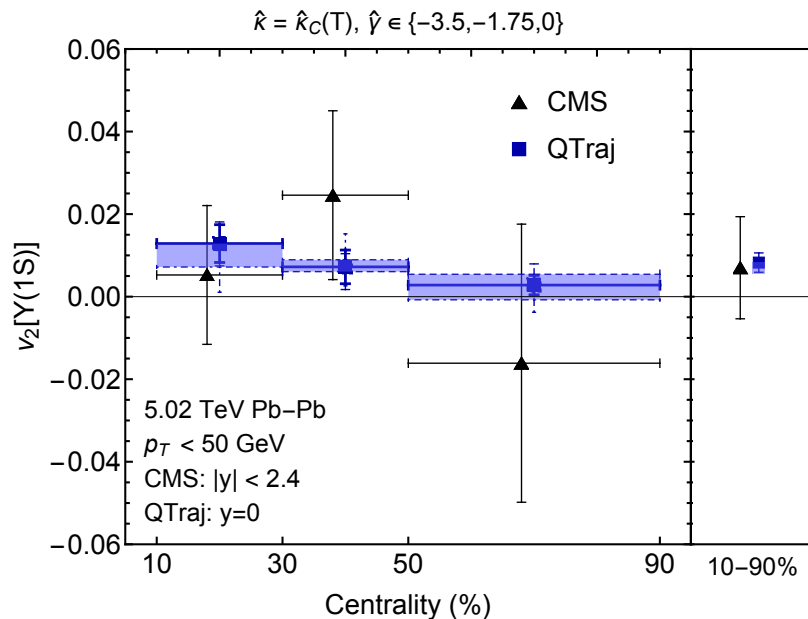
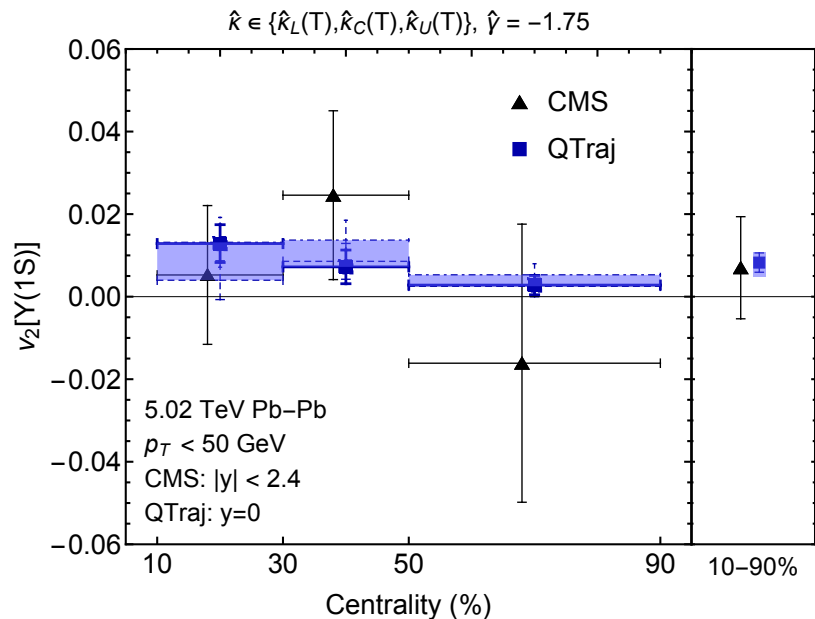
TAMU: Phys. Rev. C 96, (2017) 054901
BJS: arXiv:1809.06235

ALICE Collaboration: arXiv:1907.03169



Momentum-space anisotropies at LHC

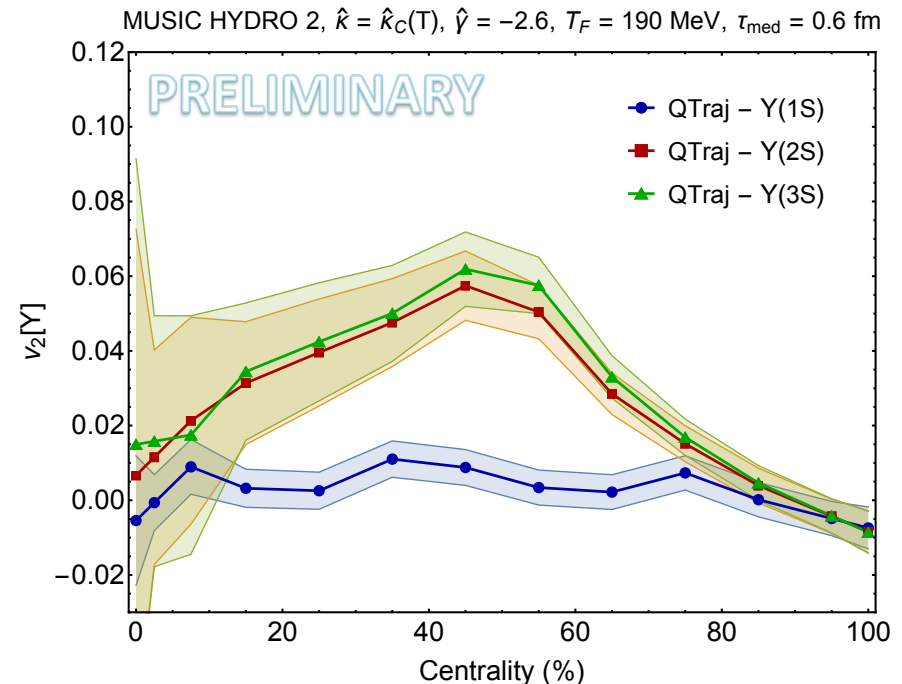
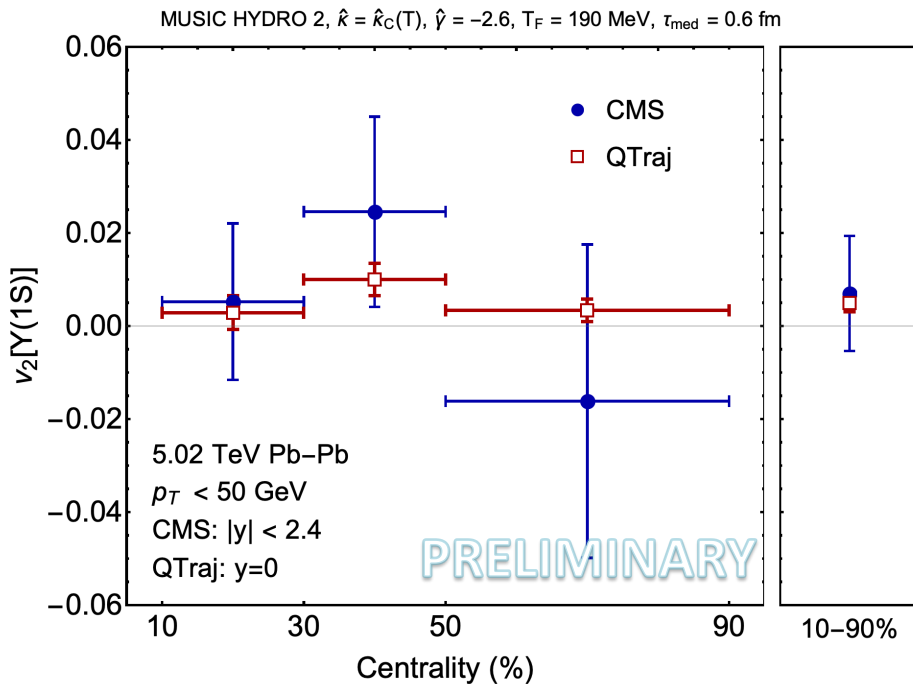
N. Brambilla, M.-A. Escobedo, M.S., A. Vairo, P. Vander Griend, and J.H. Weber, 2107.06222 (Leading-Order)



Momentum-space anisotropies at LHC

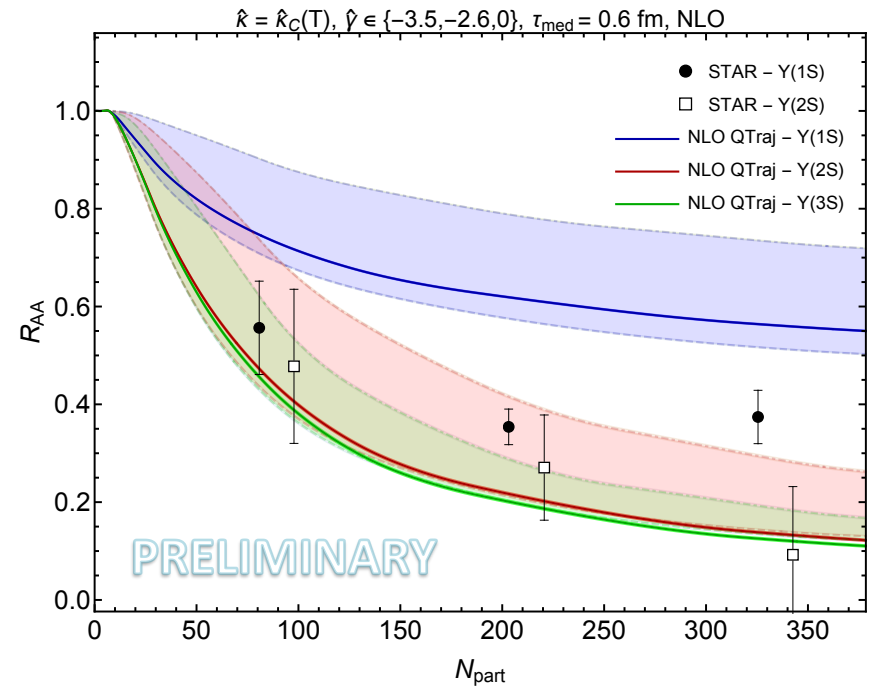
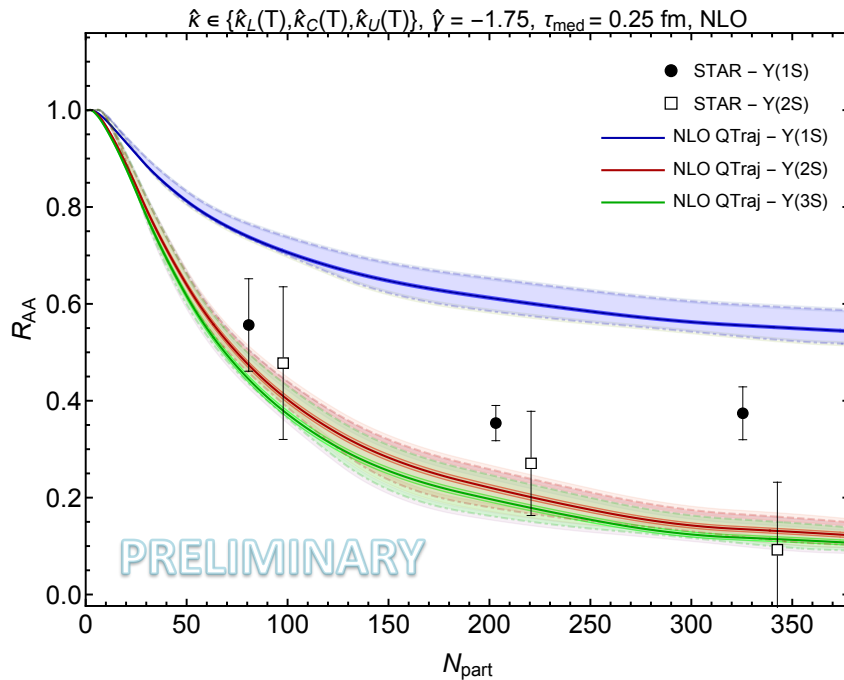
H. Alalawi, J. Boyd, and M. Strickland, forthcoming

- Forthcoming work on including the effect of fluctuating hydrodynamics.
- Using MUSIC + IPGlasma IC tuned to 5.02 TeV Pb-Pb collisions
- Agrees well with aHydro results for R_{AA} (not shown)



NLO OQS + pNRQCD predictions for R_{AA} vs N_{part} at RHIC

M. Strickland and S. Thapa, forthcoming

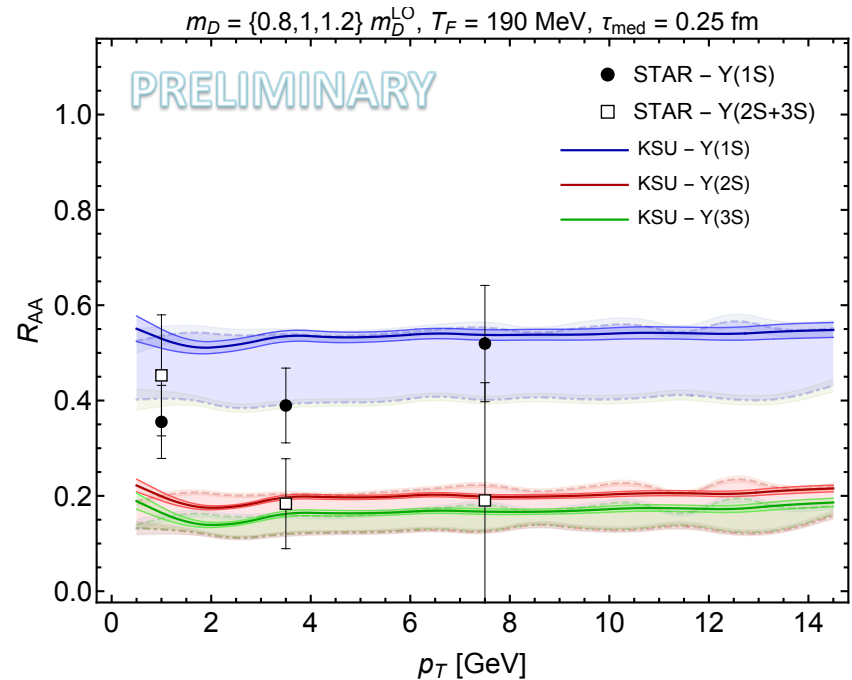
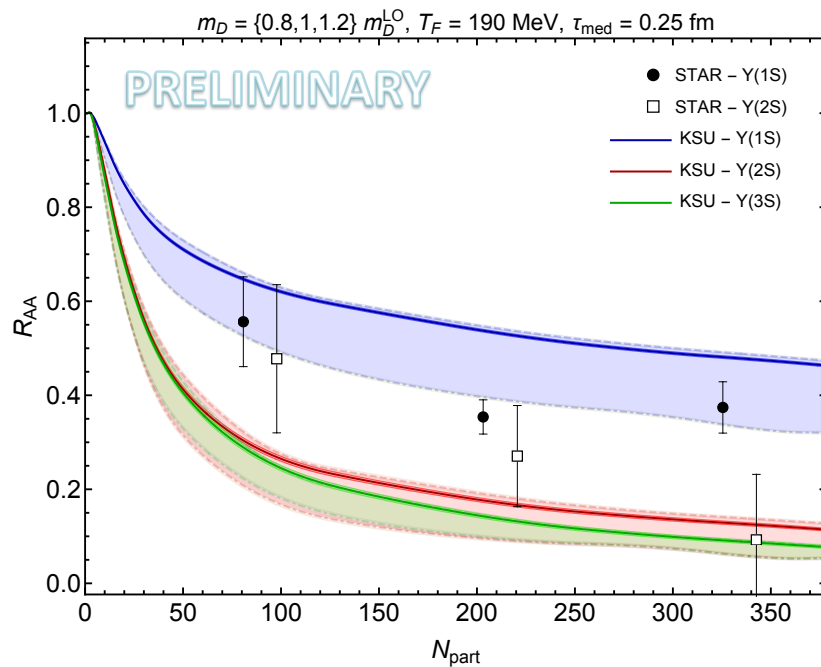


- Above are results from the NLO OQS + pNRQCD predictions for R_{AA} at 200 GeV compared to recently reported STAR data (2207.06568). Same parameters at LHC, only changed the hydrodynamic background.
- Framework does not predict enough 1S suppression
- STAR data indicate similar levels of suppression for the 1S and 2S for $N_{part} < 200$.
- Data from sPHENIX will be useful

Phenomenological KSU model RHIC predictions

A. Islam and M. Strickland, 2010.05457 and 2007.10211

M. Strickland and S. Thapa, forthcoming



- Above are results from the KSU phenomenological potential.
- It reduces to a Cornell potential with string breaking at $T=0$. Parameterization gives all observed bottomium vacuum eigenenergies to a few %. For in-medium potential the a KMS type potential is used for the real part and the Laine result for the imaginary part is used.
- The KSU model gets closer to the STAR data for the 1S, however, it can't explain the 2S results at the same time for $N_{\text{part}} < 225$. The transverse momentum dependence which is dominated by large N_{part} events, is reasonably well described.

Conclusions and Outlook

- **First 3D quantum non-abelian treatment of heavy quarkonium within the OQS+pNRQCD framework. Treatment extended to NLO in E/T.**
- Transport coefficients used were **constrained by independent lattice measurements.**
- OQS + pNRQCD works quite well in describing bottomonium suppression vs N_{part} and p_T , double ratios, and “flow” seen at LHC energies.
- However, the same setup, our preliminary results indicate that OQS + pNRQCD overpredicts $R_{AA}[1S]$ at 200 GeV when compared with recent STAR data.
- The STAR data provides a serious challenge for this approach. Could this signal that one must go beyond NLO in E/T?
- Our preliminary results indicate that the phenomenological KSU model does better in describing $R_{AA}[1S]$, however, it then underpredicts $R_{AA}[2S]$.
- Is it possible to construct a complex potential model that is (a) well founded and (b) can describe both RHIC and LHC data with a finite number of tunable parameters? It seems to be challenge at the moment.
- It will be very interesting to see what sPHENIX has to say!

Additional slides

A parallelizable approach: Quantum trajectories

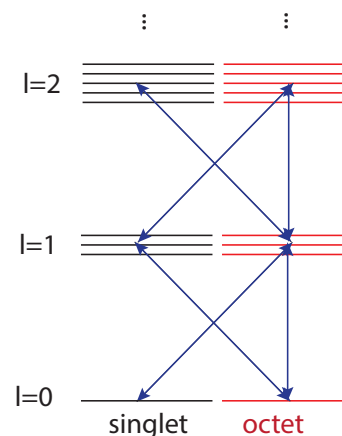
N. Brambilla, M.-A. Escobedo, M.S., A. Vairo, P. Vander Griend, and J.H. Weber, 2012.01240

$$\frac{d\rho_{\text{probe}}}{dt} = -iH_{\text{eff}}\rho_{\text{probe}} + i\rho_{\text{probe}}H_{\text{eff}}^\dagger + \sum_n C_n \rho_{\text{probe}} C_n^\dagger$$

Non-unitary “no jump” evolution

Can treat this “quantum jump” term stochastically

- Can be reduced to the solution of a large set of “quantum trajectories” in which we solve a 1D Schrödinger equation with a **non-Hermitian Hamiltonian H_{eff}** , subject to **stochastic quantum jumps**.
- The evolution with the non-Hermitian H_{eff} preserves the color and angular momentum state of the system (but not norm).
- Collapse/jump operators encode transitions between different color/angular momentum states (subject to selection rules).
- For each **physical trajectory** (path through the QGP) we average over a large set of **independent quantum trajectories** → **Embarrassingly parallel**
- **Added benefit: Can describe all angular momentum states (no cutoff) .**



How can one numerically solve these equations?

$$\frac{d\rho_{\text{probe}}}{dt} = -iH_{\text{eff}}\rho_{\text{probe}} + i\rho_{\text{probe}}H_{\text{eff}}^\dagger + \sum_n C_n \rho_{\text{probe}} C_n^\dagger$$

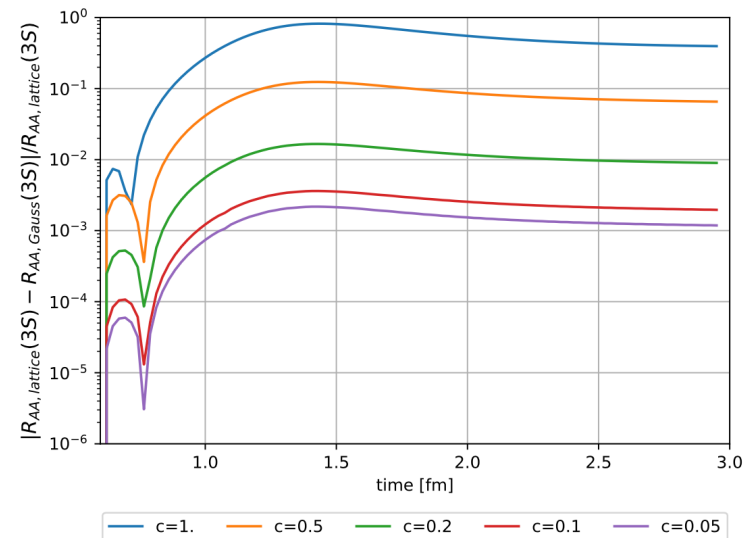
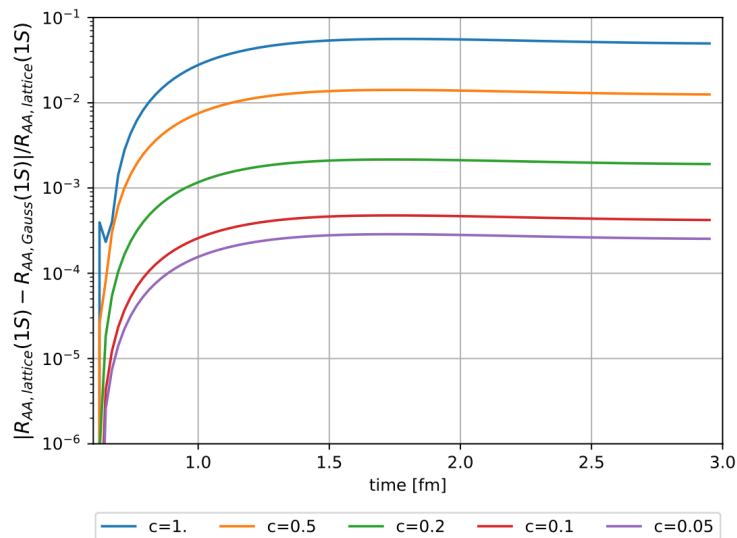
- Each block of the density matrix in color space can be decomposed into orbital angular momentum blockwise.
- Upon truncating in angular momentum ($l \leq l_{\text{max}}$) one can reduce both the singlet and octet blocks of the reduced density matrix to size $(l_{\text{max}} + 1)^2$.
- One can then discretize the radial wavefunction ($N = \#$ of lattice points) and evolve the reduced density matrix using standard differential equation and matrix solvers gives $\sim N^2(l_{\text{max}} + 1)^2$ matrix size.
- **Need to describe bound and unbound states with highly localized initial wave function, so the box must be large and have small lattice spacing \rightarrow large N and large l_{max} .**
- As N and l_{max} become large, the computation becomes very challenging.
- **Need a better/faster method which we can easily parallelize.**

Initial bottomonium wavefunction

- We took the initial wavefunction to be given by a smeared delta function (local production due to large mass, $\Delta \sim 1/M$) of the form

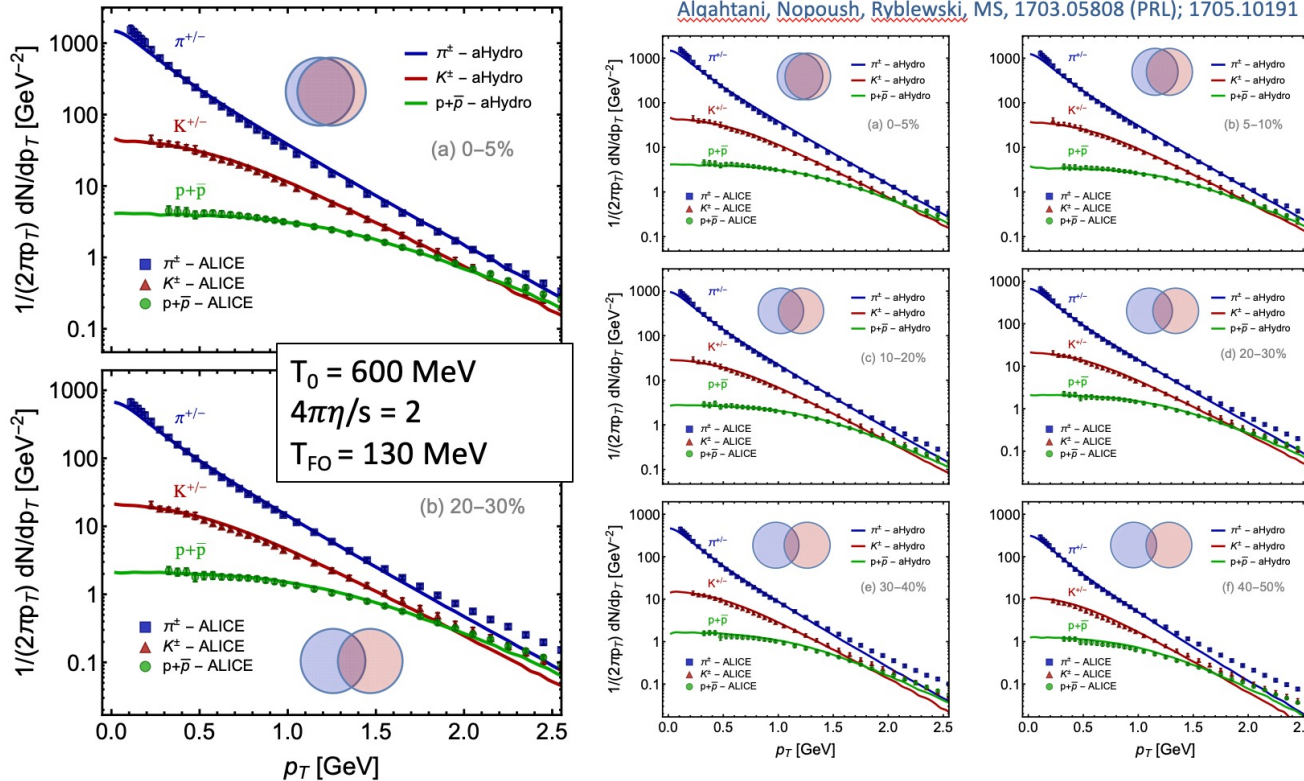
$$u_\ell(r, \tau = 0) \propto r^{\ell+1} \exp(-r^2/\Delta^2)$$

- For a given l , the **initial state is a quantum linear superposition** of the eigenstates of H.
- Includes both bound and unbound states.**
- We took $\Delta = 0.2 a_0$ which reproduces results obtained with a true delta to within 1%.



3+1D hydrodynamical background

Identified particle spectra



M. Strickland

Data are from the ALICE collaboration data for **Pb-Pb collisions @ 2.76 TeV/nucleon**

6

- We use a 3+1D dissipative code for the hydro background (quasiparticle anisotropic hydrodynamics)
- Has been tuned to RHIC and LHC heavy ion collisions
- Reproduces spectra, multiplicities, identified elliptic flow of light hadrons, HBT radii, etc.

For 5.02 TeV, $T_0 = 630 \text{ MeV}$ @ $t_0 = 0.25 \text{ fm}/c$